

# CHE/CS 537

Feb. 11 – Cell communication  
networks/Mechanistic Models

## References:

[Gerhart J.](#): 1998 Warkany lecture: signaling pathways in development. *Teratology*. 1999 Oct;60(4):226-39.

[Moon RT, Bowerman B, Boutros M, Perrimon N.](#): The promise and perils of Wnt signaling through beta-catenin. *Science*. 2002 May 31;296(5573):1644-6.

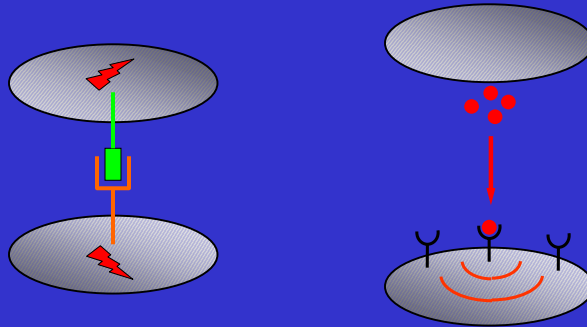
[Lee E, Salic A, Kruger R, Heinrich R, Kirschner MW.](#) The Roles of APC and Axin Derived from Experimental and Theoretical Analysis of the Wnt Pathway. *PLoS Biol*. 2003 Oct;1(1):E10.

[Aaranson DS, Horvath CM.](#): A road map for those who don't know JAK-STAT. *Science*. 2002 May 31;296(5573):1653-5. Review.

[Swameye I, Muller TG, Timmer J, Sandra O, Klingmuller U.](#) Identification of nucleocytoplasmic cycling as a remote sensor in cellular signaling by databased modeling. *Proc Natl Acad Sci U S A*. 2003 Feb 4;100(3):1028-33.

[Huang CY, Ferrell JE Jr.](#): Ultrasensitivity in the mitogen-activated protein kinase cascade. *Proc Natl Acad Sci U S A*. 1996 Sep 17;93(19):10078-83.

# Cell Communication Systems

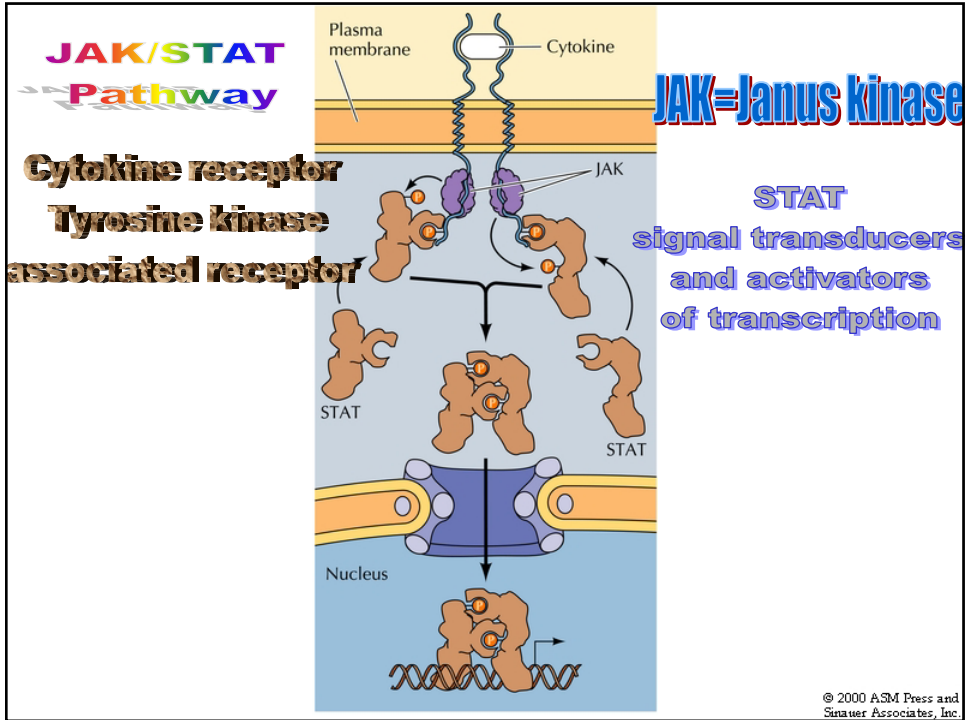


Signal Generation/Transmission/Detection/Processing

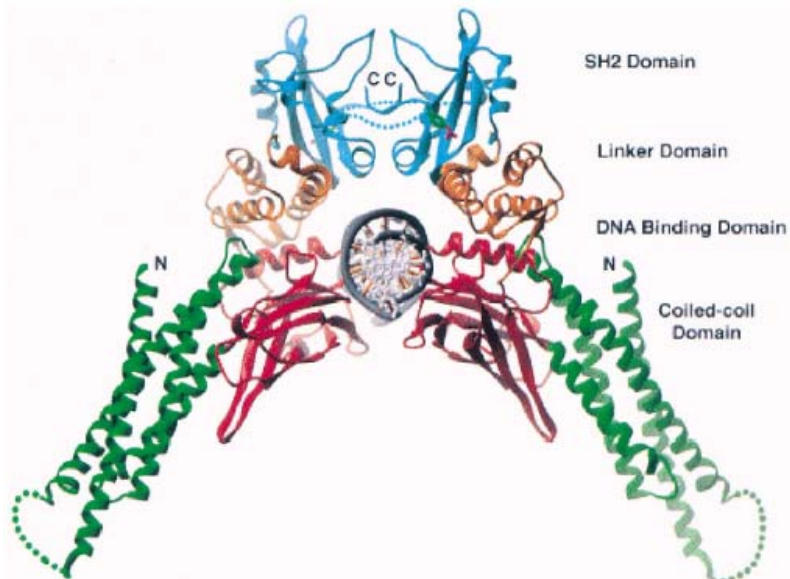
## Cell communication systems in tissue morphogenesis

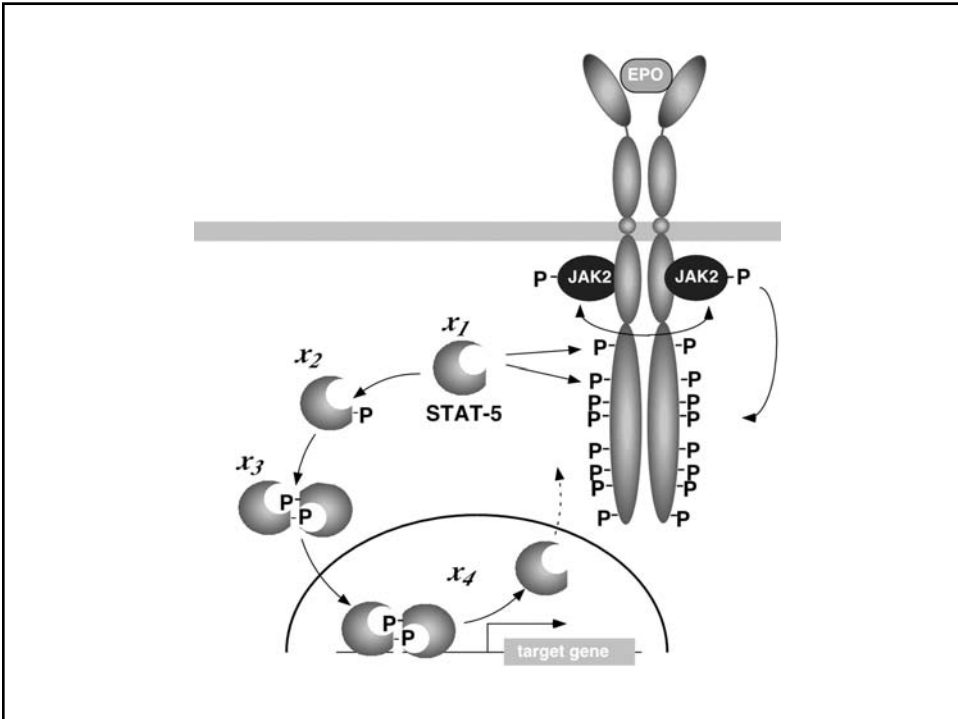
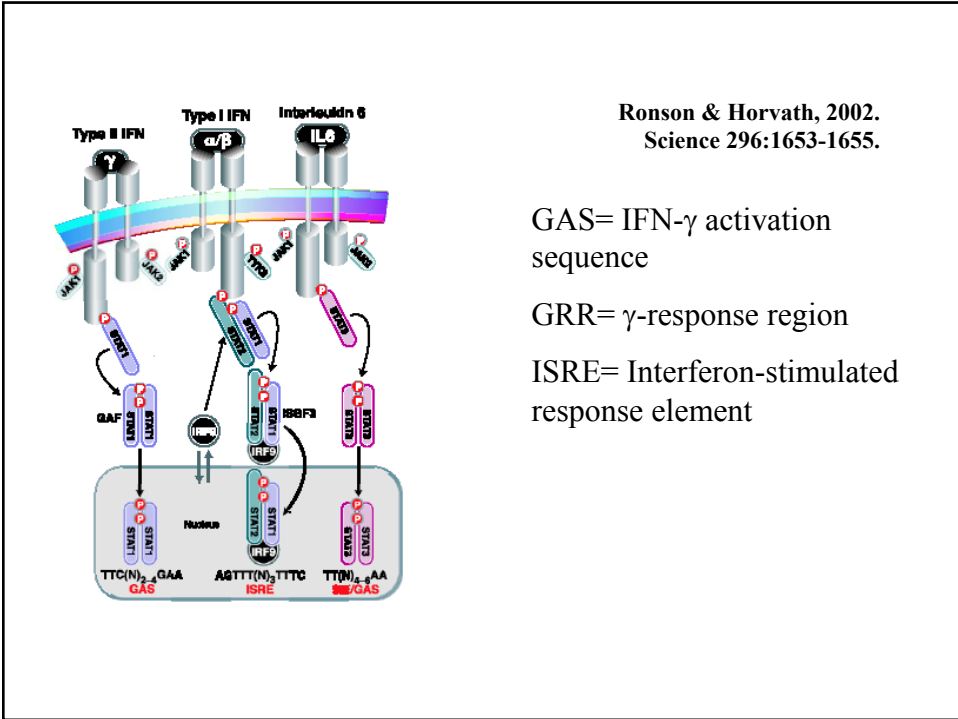
Many of the molecular players have been identified....Add a pinch of **BMP**, sprinkle some **Hedgehog**, a touch of **Wnt**, and a handful of **FGF** and you can pattern an embryo, a limb, or an organ.

(B.Z. Shilo, Cell, 2001)



## STAT1 dimer bound to DNA





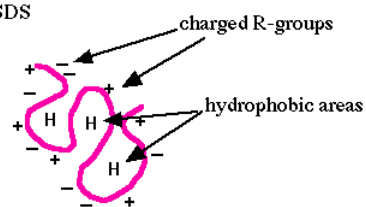
$$\dot{x}_1 = -k_1 x_1 E p o R_A \quad [ 1 ]$$

$$\dot{x}_2 = -k_2 x_2^2 + k_1 x_1 E p o R_A \quad [ 2 ]$$

$$\dot{x}_3 = -k_3 x_3 + \frac{1}{2} k_2 x_2^2 \quad [ 3 ]$$

$$\dot{x}_4 = +k_3 x_3, \quad [ 4 ]$$

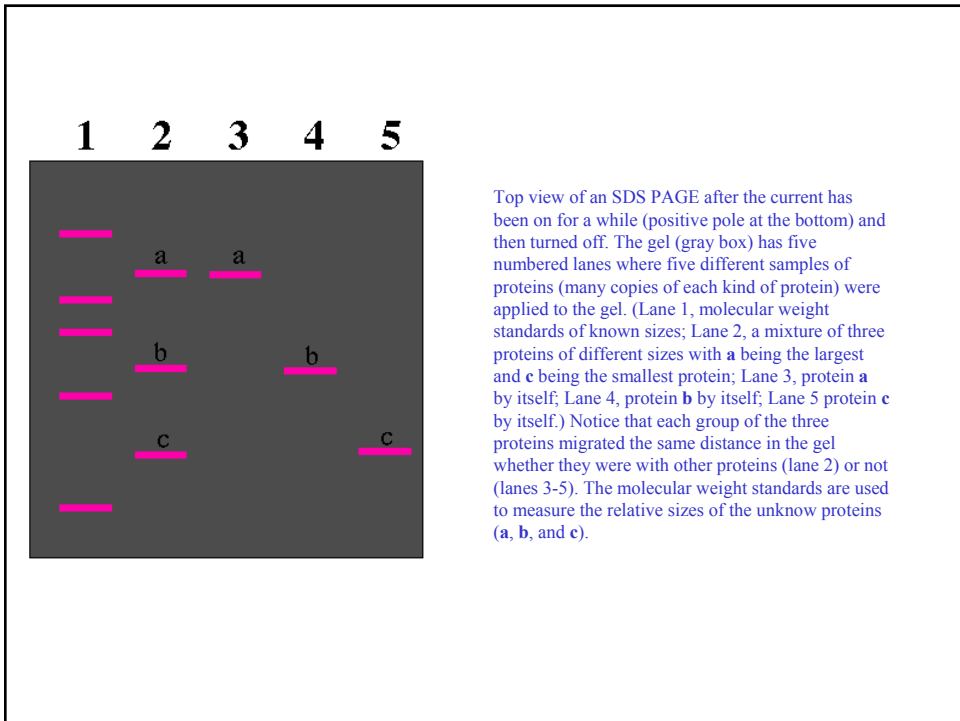
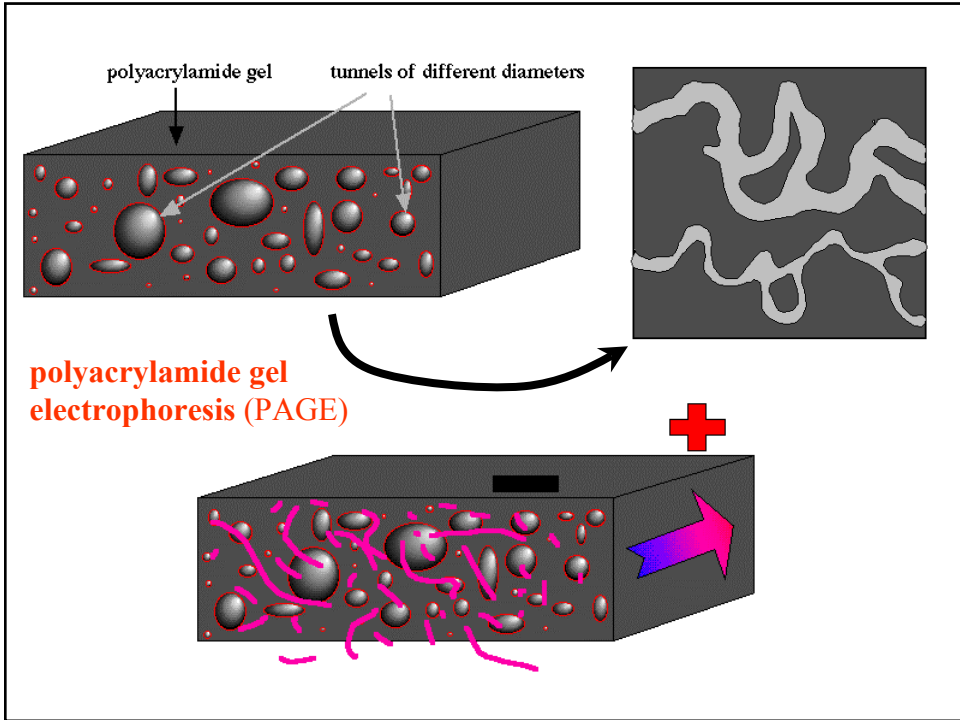
BEFORE SDS



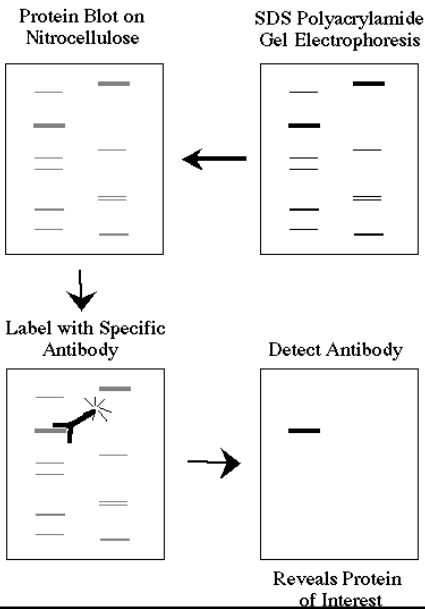
AFTER SDS



**SDS** (sodium dodecyl sulfate) is a detergent (soap) that can dissolve hydrophobic molecules but also has a negative charge (sulfate) attached to it. Therefore, if a cell is incubated with SDS, the membranes will be dissolved, all the proteins will be solubilized by the detergent, plus all the proteins will be covered with many negative charges. The end result has two important features: 1) all proteins retain only their primary structure and 2) all proteins have a large negative charge which means they will all migrate towards the positive pole when placed in an electric field.

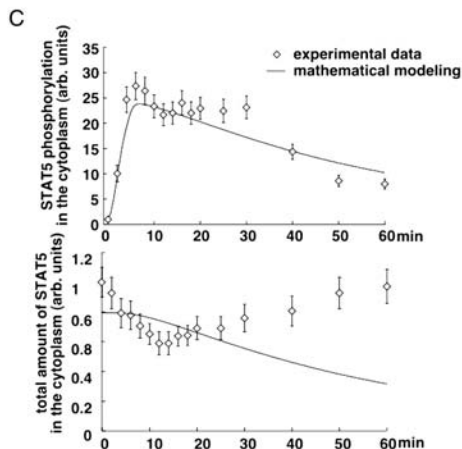
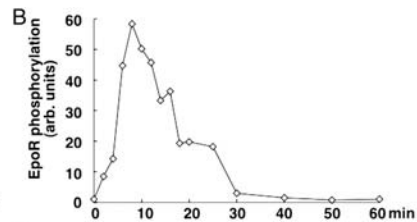
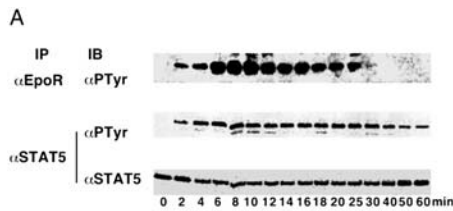


## Western Blot Procedure



Western blots allow investigators to determine the molecular weight of a protein and to measure relative amounts of the protein present in different samples.

- 1) Proteins are separated by gel electrophoresis, usually SDS-PAGE.
- 2) The proteins are transferred to a sheet of special blotting paper called nitrocellulose, though other types of paper, or membranes, can be used. The proteins retain the same pattern of separation they had on the gel.
- 3) The blot is incubated with a generic protein (such as milk proteins) to bind to any remaining sticky places on the nitrocellulose. An antibody is then added to the solution which is able to bind to its specific protein. The antibody has an enzyme (e.g. alkaline phosphatase or horseradish peroxidase) or dye attached to it which cannot be seen at this time.
- 4) The location of the antibody is revealed by incubating it with a colorless substrate that the attached enzyme converts to a colored product that can be seen and photographed.

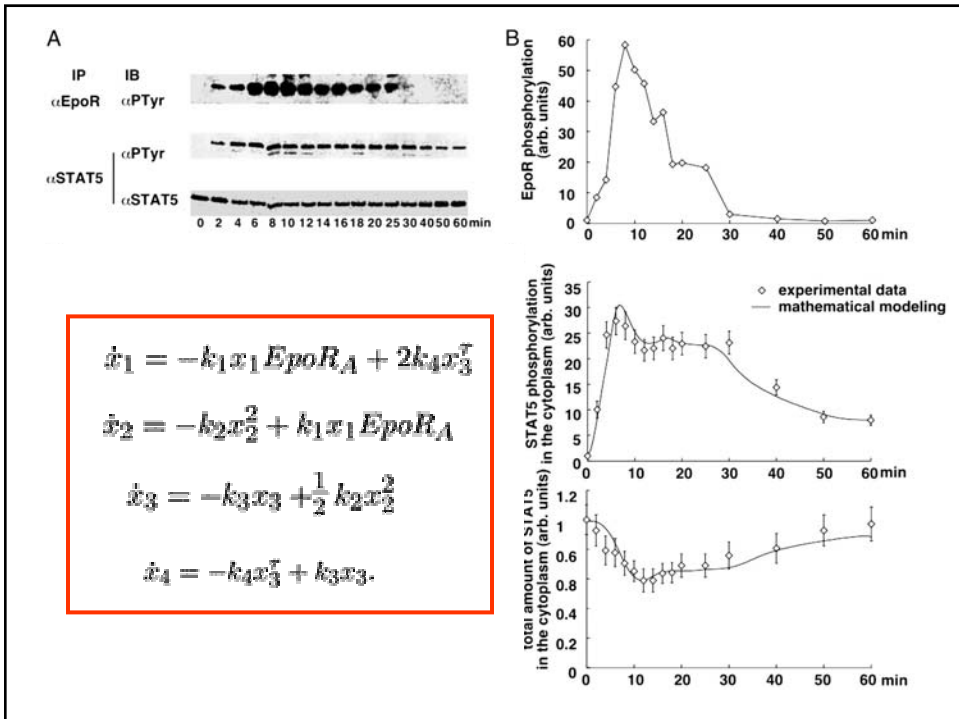
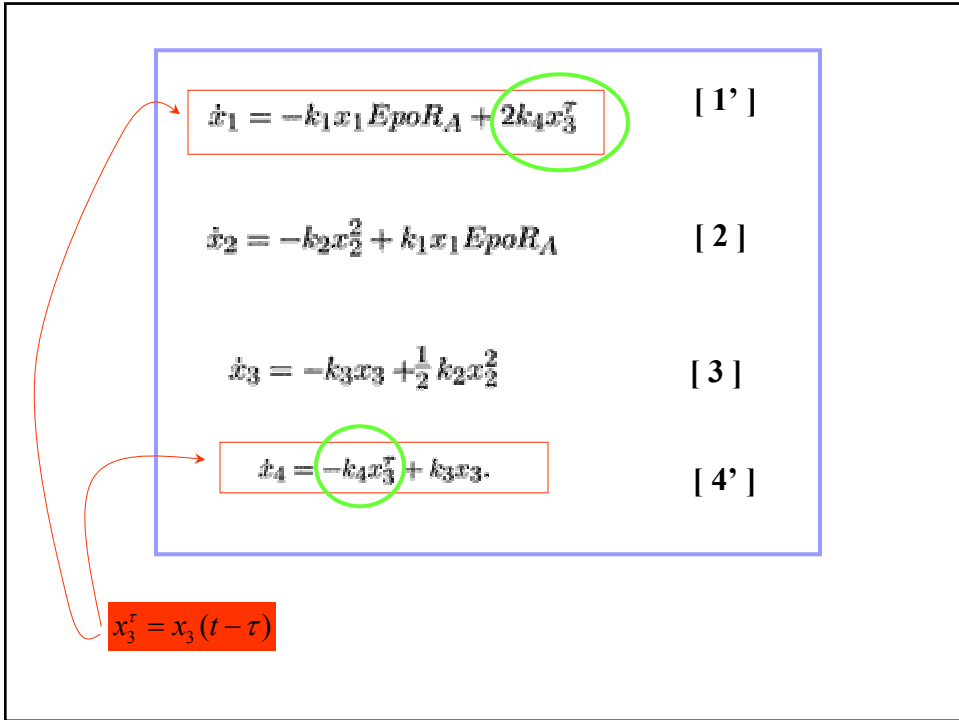


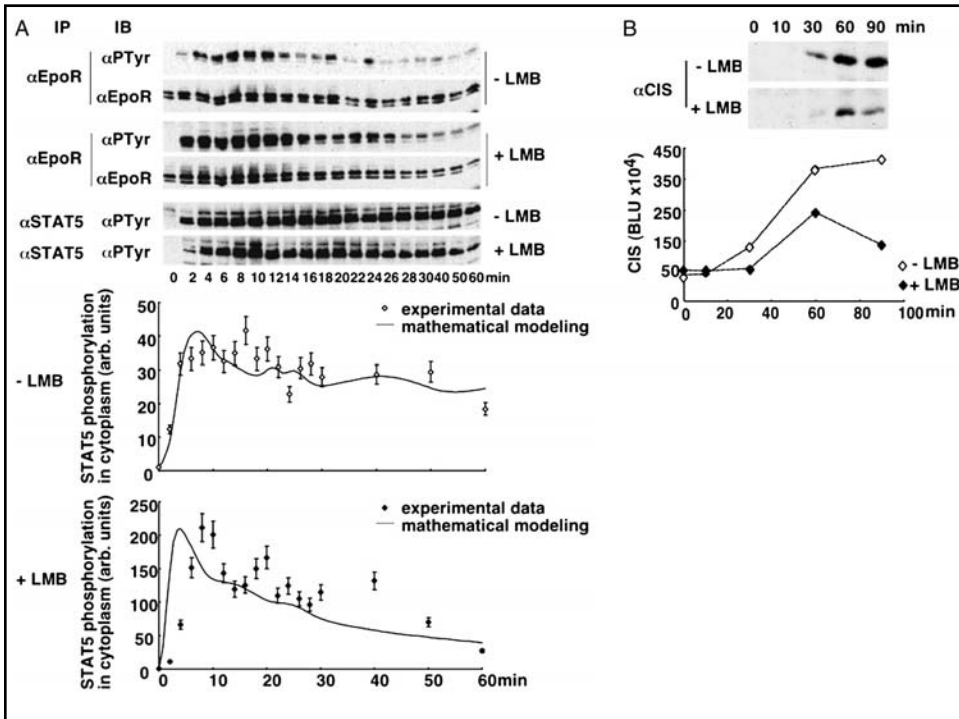
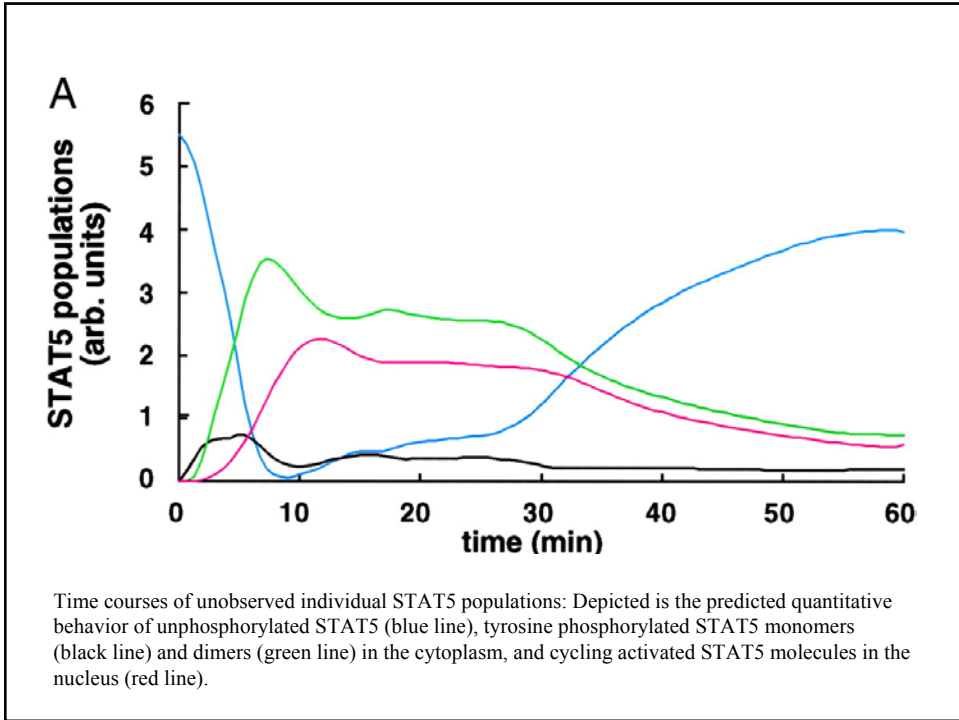
$$\dot{x}_1 = -k_1 x_1 EpoR_A$$

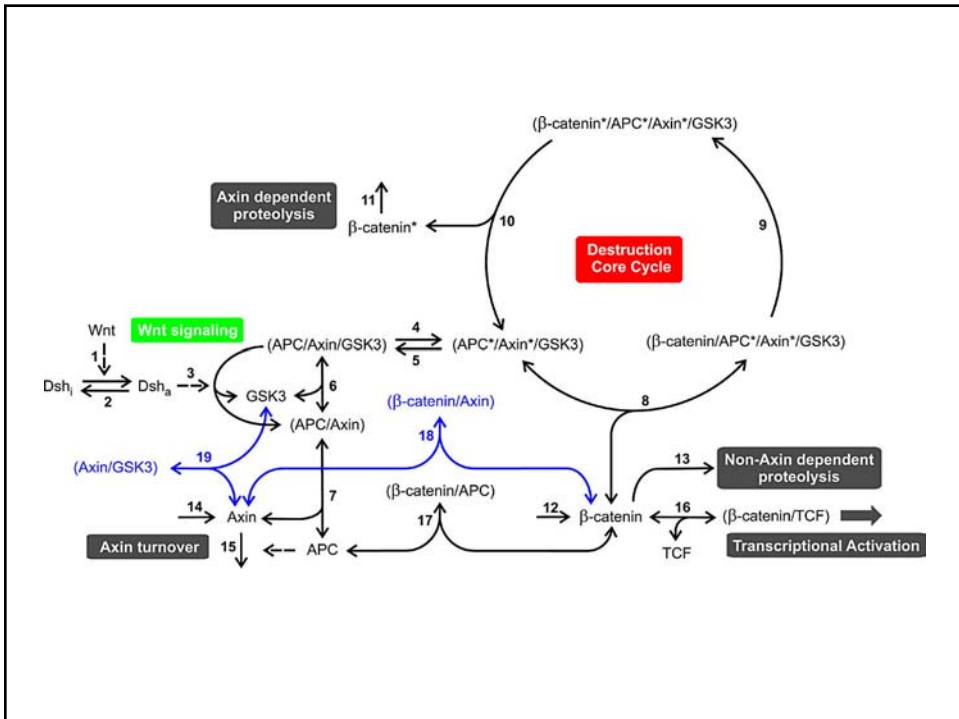
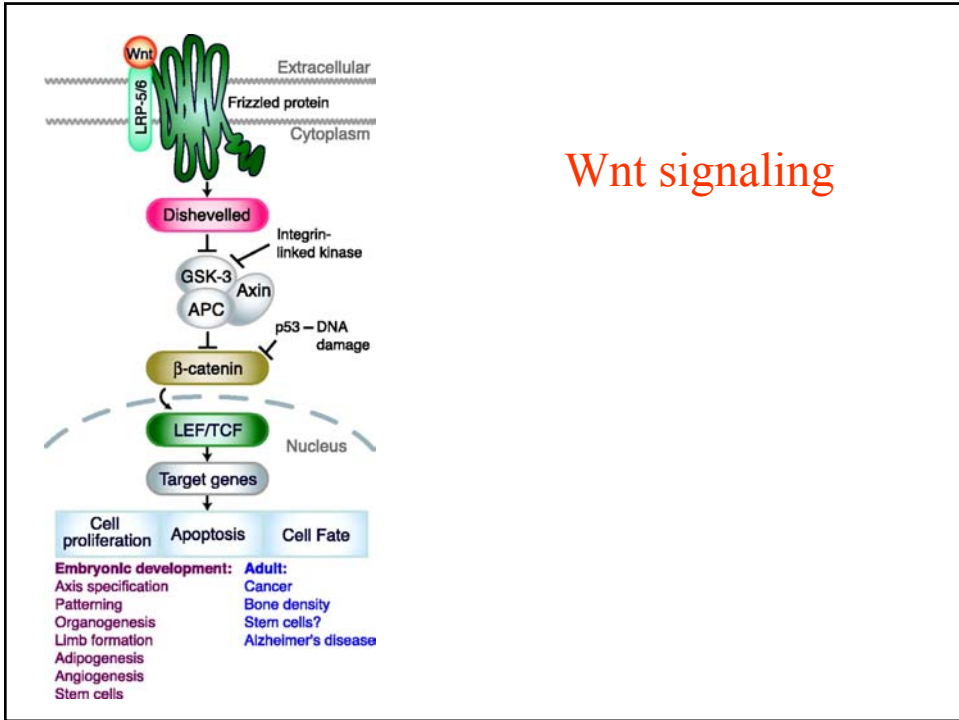
$$\dot{x}_2 = -k_2 x_2^2 + k_1 x_1 EpoR_A$$

$$\dot{x}_3 = -k_3 x_3 + \frac{1}{2} k_2 x_2^2$$

$$\dot{x}_4 = +k_3 x_3,$$



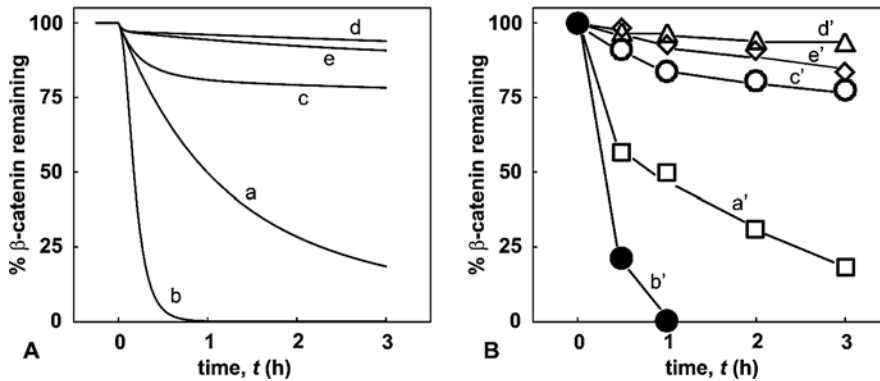




Symbol	Description	Reference value
<b>Concentrations</b>		
$Dsh^0$	total Dsh	<b>100 nM</b>
$APC^0$	total APC	<b>100 nM</b>
$TCF^0$	total TCF	<b>15 nM</b>
$GSK^0$	total GSK3 $\beta$	<b>50 nM</b>
$Axin^0$	total axin	<b>0.02 nM</b>
$\beta\text{-catenin}^0$	total $\beta$ -catenin	<b>35 nM</b>
$\beta\text{-catenin}^*$	free phosphorylated $\beta$ -catenin	<i>1 nM</i>
<b>Dissociation constants</b>		
$K_6$	binding of GSK3 $\beta$ to (APC/axin)	<i>10 nM</i>
$K_7$	binding of APC to axin	<i>50 nM</i>
$K_8$	binding of $\beta$ -catenin to (APC/axin/GSK3 $\beta$ )	<i>120 nM</i>
$K_{16}$	binding of $\beta$ -catenin to TCF	<i>30 nM</i>
$K_{17}$	binding of $\beta$ -catenin to APC	<i>1200 nM</i>
<b>Concentration ratios</b>		
$\frac{(APC^*/Axin^*/GSK3\beta)}{(APC/Axin/GSK3\beta)}$		2
$\frac{(\beta\text{-catenin}^*/APC^*/Axin^*/GSK3\beta)}{(\beta\text{-catenin}/APC^*/Axin^*/GSK3\beta)}$		1
<b>Flux and flux ratio</b>		
$v_{11}$	degradation flux of $\beta$ -catenin via the proteasome	<b>25 nM/h</b>
$v_{12}/v_{11}$		<b>0.015</b>
<b>Characteristic times</b>		
$\tau_{CP}$	phosphorylation/dephosphorylation of APC and axin	<i>2.5 min</i>
$\tau_{GSK,ass}$	GSK3 $\beta$ association/dissociation	<i>1 min</i>
$\tau_{ax,deg}$	Axin degradation	<b>6 min</b>

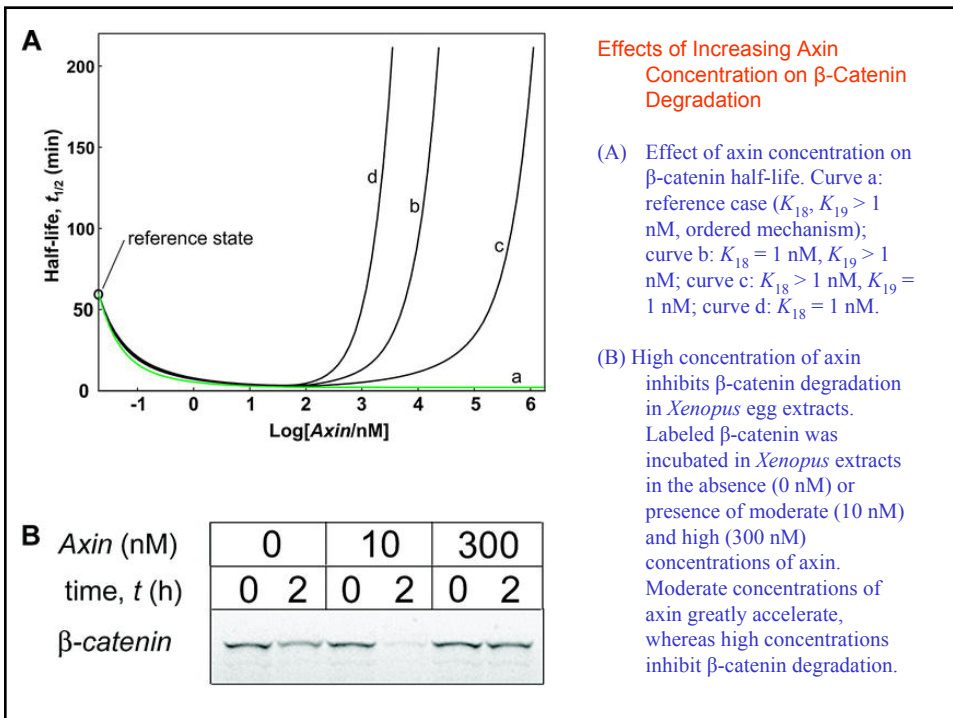
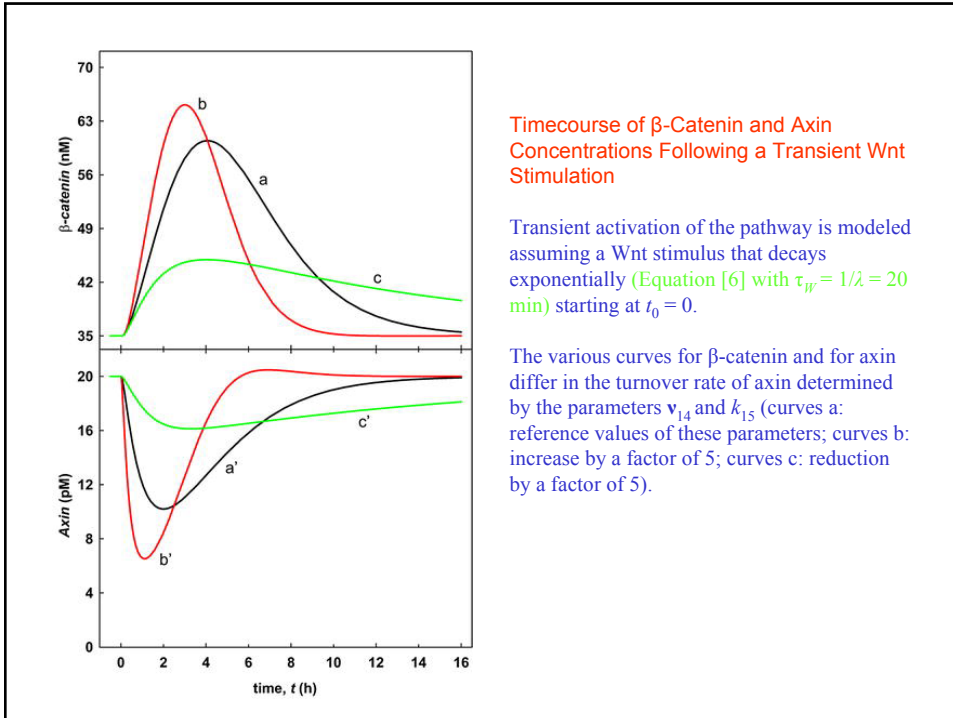
The data are grouped into concentrations of pathway components, dissociation constants of protein complexes, concentration ratios, fluxes and ux ratios, and characteristic times of selected processes. Experimental evidence for these data is discussed in the text. From these data, the following rates and rate constants are calculated:  $v_{12} = 0.42 \text{ nM} \cdot \text{min}^{-1}$  (rate of  $\beta$ -catenin synthesis),  $v_{14} = 8.2 \cdot 10^{-7} \cdot \text{nM} \cdot \text{min}^{-1}$  (rate of axin synthesis),  $k_4 = 0.27 \text{ min}^{-1}$ ,  $k_5 = 0.13 \text{ min}^{-1}$ ,  $k_6 = 9.1 \cdot 10^{-2} \text{ nM}^{-1} \cdot \text{min}^{-1}$ ,  $k_8 = 0.91 \text{ nM}^{-1} \cdot \text{min}^{-1}$ ,  $k_9 = 210 \text{ min}^{-1}$ ,  $k_{10} = 210 \text{ min}^{-1}$ ,  $k_{11} = 0.42 \text{ min}^{-1}$ ,  $k_{12} = 2.6 \cdot 10^{-6} \text{ min}^{-1}$ ,  $k_{13} = 0.17 \cdot \text{min}^{-1}$ . See Table S2, found at <https://dx.doi.org/10.1371/journal.pbio.0000010.s002>, for more precise numbers used in the calculations.  
**Bold: Measured values, Italics:** Estimated values.  
 DOI: 10.1371/journal.pbio.0000010.t001

## Response to perturbation in protein synthesis in different backgrounds



(A) Simulated timecourses of  $\beta$ -catenin degradation. In vitro conditions are simulated by switching off synthesis of  $\beta$ -catenin and axin ( $v_{12} = 0$ ,  $v_{14} = 0$  for  $t > 0$ ). Curve a: reference case (no addition of further compounds); curve b: addition of 0.2 nM axin; curve c: addition of 1  $\mu$ M activated Dsh (deactivation of Dsh was neglected,  $k_2 = 0$ ); curve d: inhibition of GSK3 $\beta$  (simulated by setting  $k_4 = 0$ ,  $k_9 = 0$ ); curve e: addition of 1  $\mu$ M TCF. Addition of compounds (axin, Dsh, TCF) and inhibition of GSK3 $\beta$  was performed at  $t = 0$ .

(B) Experimental timecourse of  $\beta$ -catenin degradation in *Xenopus* egg extracts in the presence of buffer (curve a'), axin (curve b': 10 nM), Dsh (curve c': 1  $\mu$ M), Li<sup>+</sup> (curve d': 25 mM), or Tcf3 (curve e': 1  $\mu$ M).



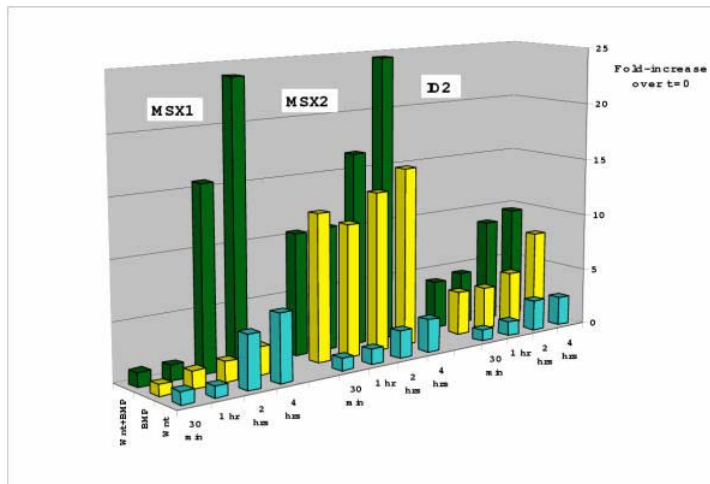
Control coefficient:  
At steady state

$$C_j^{\beta-Cat} = \frac{p_j}{\beta - Cat} \frac{\partial \beta - Cat}{\partial p_j}$$

	W = 0		W = 1	
	$C_j^{\beta cat}$	$C_j^{axin}$	$C_j^{\beta cat}$	$C_j^{axin}$
APC	-0.83	0.79	-0.87	0.52
GSK3 $\beta$	-0.89	0.74	-0.94	0.40
PP2A	0.89	-0.50	0.94	-0.30
TCF	0.20	0	0.07	0
Dsh	0	0	0.78	-0.33
$\beta$ -catenin	1.00	0.20	1.00	0.44
Axin	-1.08	1.00	-1.59	1.00

The control coefficients were obtained by numerical determination of the response to a change of total concentrations by 1%. Coefficients are given for the reference state and for the standard stimulated state.  
DOI: 10.1371/journal.pbio.0000010.t004

### Wnt-induced gene expression



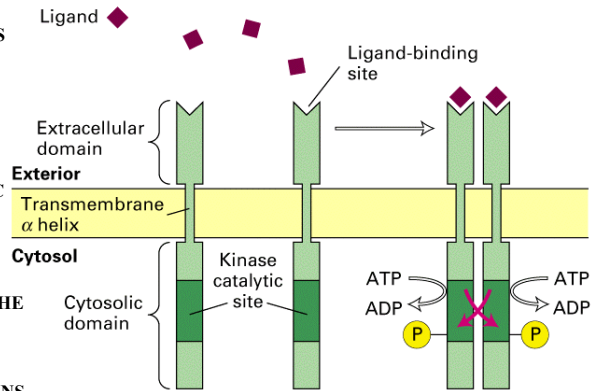
Notice the time scale of transcriptional response

# GENERAL STRUCTURE AND ACTIVATION OF RECEPTOR TYROSINE KINASES (RTKS)

AS WITH THE EPO RECEPTOR, LIGAND BINDING INDUCES A CONFORMATIONAL CHANGE THAT PROMOTES OR STABILIZES RECEPTOR DIMERS.

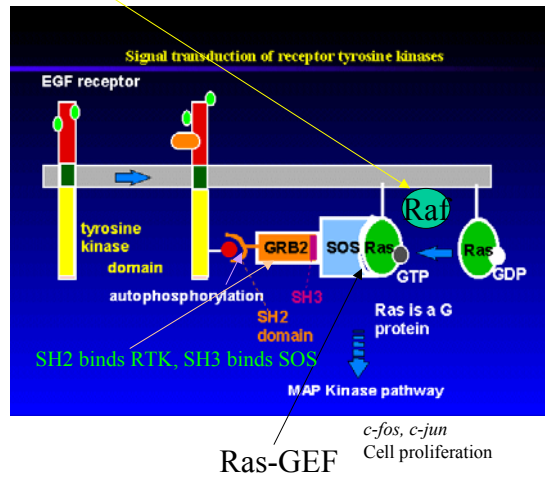
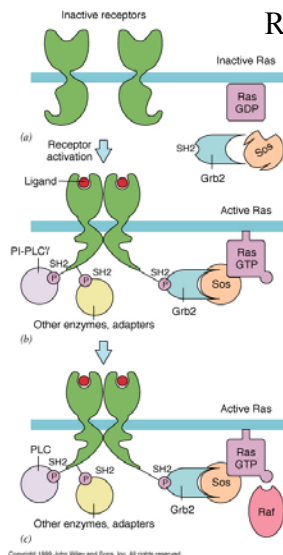
THE KINASE ACTIVITY OF EACH SUBUNIT OF THE DIMERIC RECEPTOR INITIALLY PHOSPHORYLATES TYROSINE RESIDUES NEAR THE CATALYTIC SITE IN THE OTHER SUBUNIT, CAUSING ITS ACTIVATION.

SUBSEQUENTLY, TYROSINE RESIDUES IN OTHER PARTS OF THE CYTOSOLIC DOMAIN BECOME PHOSPHORYLATED AND SERVE AS DOCKING SITES FOR SH2 DOMAINS OF SIGNALING PROTEINS

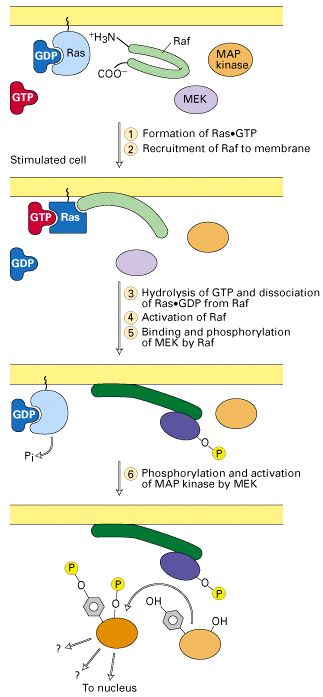


Steps in the activation of Ras by RTKs. Fig. 15.24

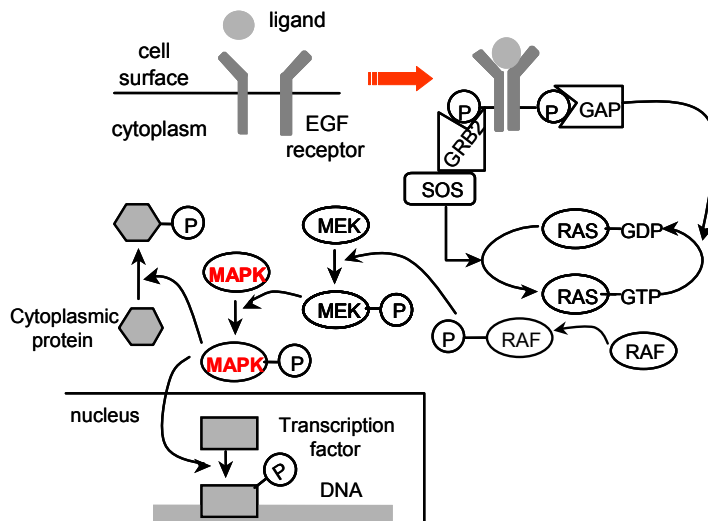
Raf is a PK that triggers MAP-K pathway



# Kinase cascade that transmits signals downstream from activated Ras protein



# Ligand-binding initiates a cascade of events



# MAPK activity can be followed

- In time
- And space

Main tool: phosphorylation state-specific antibodies – recognize phosphorylated amino acids in the context of a specific surrounding aminoacid sequence

## Experimental analysis of MAPK dynamics (1)

344

ASTHAGIRI, HORWITZ, AND LAUFFENBURGER

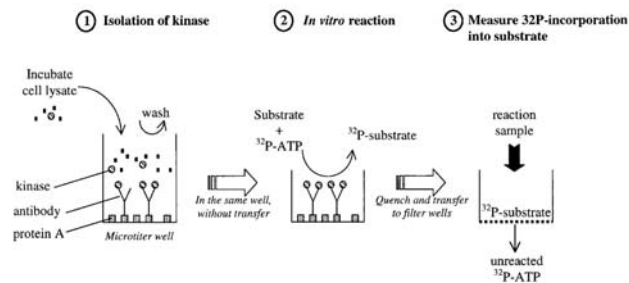


**FIG. 1.** This kinase activity assay preserves a 96-well format through the entire procedure allowing high throughput. A kinase activity assay can be partitioned into three general steps: (i) the isolation of the kinase from the other cell lysate proteins, (ii) an *in vitro* reaction in which the protein substrate is phosphorylated by the kinase, and (iii) the recovery of the phosphorylated substrate and quantification of the degree of phosphorylation as a measure of kinase activity. In the first step of this assay, an antibody that recognizes the kinase is used to isolate it. The antibody is coated in the well in the proper orientation through its interaction with protein A, which is covalently bound to the well surface. The second reaction step is performed in the same microtiter well in which the kinase was isolated. After quenching the reaction, the third step of recovering the phosphorylated substrate is performed by filtering a sample from the reaction through a 96-well plate fitted with a phosphocellulose membrane. This membrane captures the phosphorylated substrate and allows unreacted ATP to pass through. The filters are then punched out and scintillation counted to determine the amount of  $^{32}\text{P}$  incorporation into the protein substrate.

## Experimental analysis of MAPK dynamics (2)

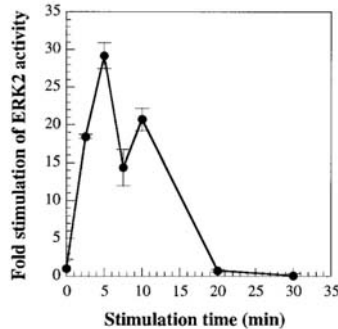
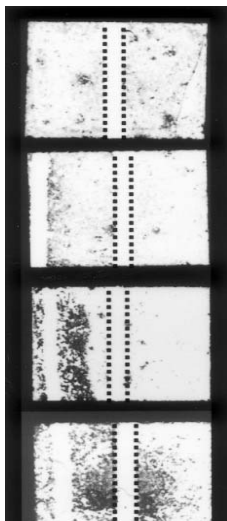


**FIG. 7.** Time-course of ERK2 activity in CHO cells in response to 15 nM EGF stimulation. CHO cells were stimulated with 15 nM EGF and were lysed at different time points. ERK2 activity in each cell lysate was measured and subtracted from background activity measured in plain lysis buffer. The background-adjusted ERK2 activity was normalized to the ERK2 activity immediately following serum starvation (i.e., the zero time point).

## Spatially resolved pattern of MAPK phosphorylation (1)



**pre-lesion**

**2'**

**10'**

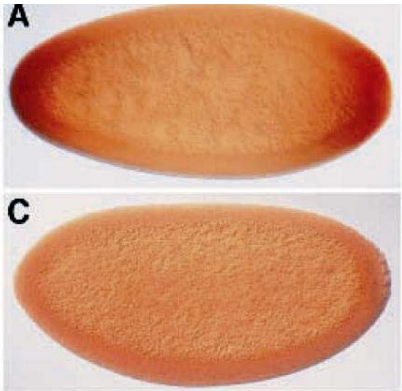
**30'**

Figure 3. Intercellular spread of ERK/MAPK activation can cross a wide cell-free barrier. A cell-free barrier (400-800 m wide) was created by making a central vertical lesion in the monolayer 24 h prior to the experimental lesion (dashed double line).

Mandell JW, Gocan NC, Vandenberg SR.  
Mechanical trauma induces rapid astroglial activation of ERK/MAP kinase:  
Evidence for a paracrine signal.  
Glia. 2001 Jun;34(4):283-95.

# Spatially resolved pattern of MAPK phosphorylation (2)

## immunohistochemistry

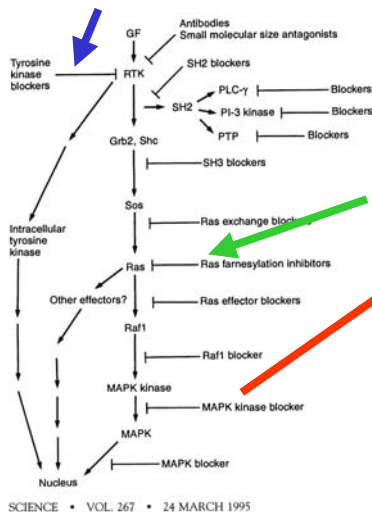


Gabay L, Seger R, Shilo BZ. MAP kinase in situ activation atlas during Drosophila embryogenesis. *Development*. 1997 Sep;124(18):3535-41.

MAP kinase (ERK) is activated by dual phosphorylation of threonine and tyrosine residues by MEK (1). A monoclonal antibody, termed diphospho-ERK (dp-ERK), was raised against a dually phosphorylated 11-amino acid peptide that constitutes the vertebrate ERK activation loop (11-13). All 11 residues are conserved in the single Drosophila ERK homolog Rolled (14), raising the possibility of cross-reactivity.

Positive staining with a dp-ERK antibody is not itself indicative of functional activation

## Pharmacological Inhibitors of MAPK signaling



SCIENCE • VOL. 267 • 24 MARCH 1995

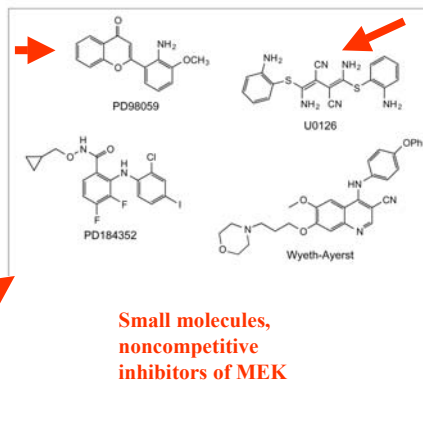
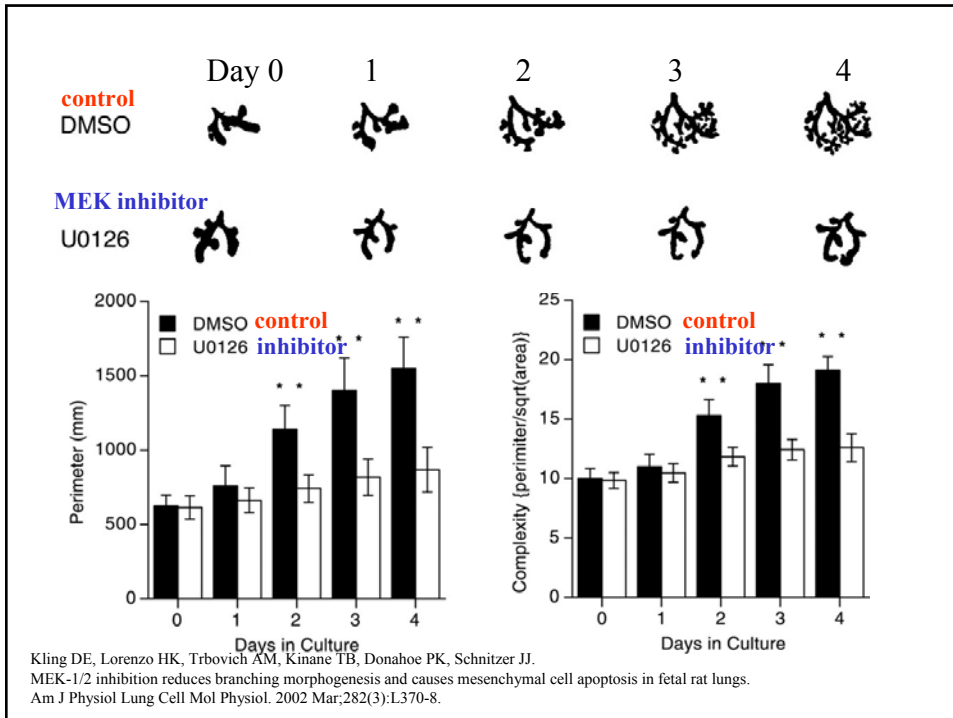


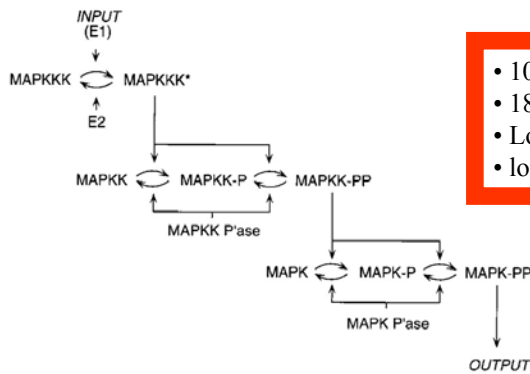
Fig. 2. Mitogen-activated protein kinase (MAPK)/extracellular signal-regulated kinase (ERK) kinase (MEK) inhibitors. PD98059, PD184352 and U0126 are noncompetitive inhibitors of MEK1 and MEK2. The Wyeth-Ayerst compound is reported to inhibit active MEK1. Ro92210, LL216402 and L783277 are compounds isolated from microorganisms. Ro92210 and LL216402 are inhibitors of MEK1 and MEK2 that compete with ATP. L783277 has a similar structure to Ro92210 and LL216402. L783277 is reported to inhibit Jun-N-terminal kinase (JNK)/p38 MAPK pathways upstream of MAPK, but a direct in vitro assay of MEK inhibition has not been reported.

English JM, Cobb MH. Pharmacological inhibitors of MAPK pathways. *Trends Pharmacol Sci*. 2002 Jan;23(1):40-5. Review



## Quantitative analysis of MAPK cascades

- Steady states (switch-like behavior)
- Dynamics (specificity in signaling)



- 10 reactions
- 18 rate equations
- Lots of parameters
- looooots of typos in the paper too

FIG. 1. Schematic view of the MAPK cascade. Activation of MAPK depends upon the phosphorylation of two conserved sites [Thr-183 and Tyr-185 in rat p42 MAPK/Erk2 (4, 5)]. Full activation of MAPKK also requires phosphorylation of two sites [Ser-218 and Ser-222 in mouse Mek-1/MKK1 (6–10)]. Detailed mechanisms for the activation of various MAPKKKs (e.g., Raf-1, B-Raf, Mos) are not yet established; here we assume that MAPKKKs are activated and inactivated by enzymes we denote E1 and E2. MAPKKK\* denotes activated MAPKKK. MAPKK-P and MAPKK-PP denote singly and doubly phosphorylated MAPKK, respectively. MAPK-P and MAPK-PP denote singly and doubly phosphorylated MAPK. P'ase denotes phosphatase.

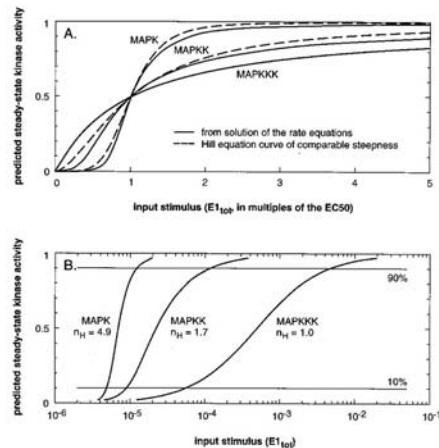


FIG. 2. Predicted stimulus/response curves for MAPK cascade components calculated by numerical solution of the rate equations for the MAP kinase cascade. (A) Predicted responses (solid lines) on a linear plot. The input stimulus is expressed in multiples of the  $EC_{50}$ , the concentration of  $E1_{100}$  that produces a 50% maximal response. The dashed lines are Hill equation curves whose steepness (the ratio of their  $EC_{90}$  to  $EC_{10}$ ) is the same as the steepness of the calculated curves. (B) A semi-logarithmic plot of the predicted responses. Here the input stimulus ( $E1_{100}$ ) is expressed in absolute, rather than relative, terms.

Enzyme	Range of assumed concentrations	Range of effective Hill coefficients (nH) predicted for		
		MAPKKK	MAPKK	MAPK
MAPKKK	0.6–15 nM (3 nM <sup>†</sup> )	0.9–1.0	1.6–1.7	3.8–5.1
MAPKK	0.24–6 μM (1.2 μM <sup>†</sup> )	1.0	1.4–1.9	2.4–9.1
MAPK	0.24–6 μM (1.2 μM <sup>†</sup> )	1.0	1.7	3.8–5.1
E2 (MAPKKK inactivase)	0.06–1.5 nM	1.0	1.7	4.9
MAPKK P <sup>ase</sup>	0.06–1.5 nM	1.0–1.1	1.6–1.7	3.8–5.1
MAPK P <sup>ase</sup>	24–600 nM	1.0	1.6–1.7	2.5–5.1

The assumed concentrations of each enzyme were individually varied over the ranges shown, with the assumed concentrations of the other five enzymes held constant. The effective Hill coefficients were calculated from the steepness of the predicted stimulus/response curves, as described in the text.

<sup>†</sup>The numbers shown in parentheses are estimated values for the concentrations of Mos (a MAPKKK), Mek-1 (a MAPKK), and p42 MAPK (a MAPK) in *Xenopus* oocytes. We initially assumed [E2] to be 0.3 nM, [MAPKK P<sup>ase</sup>] to be 0.3 nM, and [MAPK P<sup>ase</sup>] to be 120 nM. See text for details.

Table 2. Predicted Hill coefficients for MAP kinase cascade components: Varying the assumed  $K_m$  values

Reaction	Range of assumed $K_m$ values	Range of effective Hill coefficients (nH) predicted for		
		MAPKKK	MAPKK	MAPK
1. MAPKKK → MAPKKK*	60–1500 nM	1.0	1.7	4.9
2. MAPKKK* → MAPKKK	60–1500 nM	1.0	1.7	4.9
3. MAPKK → MAPKK-P	60–1500 nM	1.0	1.3–2.3	4.0–5.1
4. MAPKK-P → MAPKK	60–1500 nM	1.0	1.5–1.9	3.6–6.7
5. MAPKK-P → MAPKK-PP	60–1500 nM	1.0	1.3–2.4	3.8–5.2
6. MAPKK-PP → MAPKK-P	60–1500 nM	1.0	1.7–1.8	4.1–6.4
7. MAPK → MAPK-P	60–1500 nM (300 nM <sup>†</sup> )	1.0	1.7	3.7–6.2
8. MAPK-P → MAPK	60–1500 nM	1.0	1.7	4.3–5.2
9. MAPK-P → MAPK-PP	60–1500 nM	1.0	1.7	3.4–6.1
10. MAPK-PP → MAPK-P	60–1500 nM	1.0	1.7	4.7–5.1

The assumed  $K_m$  values for each reaction were individually varied over the ranges shown, with the assumed  $K_m$  values for the other nine reactions held constant. The effective Hill coefficients were calculated from the steepness of the predicted stimulus/response curves, as described in the text.

<sup>†</sup>The  $K_m$  value for reaction 7 has been measured to be 300 nM for the phosphorylation of a mammalian MAPK by a MAPKK (N. Ahn, personal communication). All of the other  $K_m$  values were initially assumed to be 300 nM as well.

Table 2. Predicted Hill coefficients for MAP kinase cascade components: Varying the assumed  $K_m$  values

Reaction	Range of assumed $K_m$ values	Range of effective Hill coefficients (nH) predicted for		
		MAPKKK	MAPKK	MAPK
1. MAPKKK → MAPKKK*	60–1500 nM	1.0	1.7	4.9
2. MAPKKK* → MAPKKK	60–1500 nM	1.0	1.7	4.9
3. MAPKK → MAPKK-P	60–1500 nM	1.0	1.3–2.3	4.0–5.1
4. MAPKK-P → MAPKK	60–1500 nM	1.0	1.5–1.9	3.6–6.7
5. MAPKK-P → MAPKK-PP	60–1500 nM	1.0	1.3–2.4	3.8–5.2
6. MAPKK-PP → MAPKK-P	60–1500 nM	1.0	1.7–1.8	4.1–6.4
7. MAPK → MAPK-P	60–1500 nM (300 nM <sup>†</sup> )	1.0	1.7	3.7–6.2
8. MAPK-P → MAPK	60–1500 nM	1.0	1.7	4.3–5.2
9. MAPK-P → MAPK-PP	60–1500 nM	1.0	1.7	3.4–6.1
10. MAPK-PP → MAPK-P	60–1500 nM	1.0	1.7	4.7–5.1

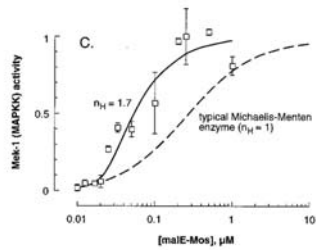
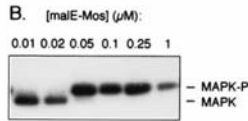
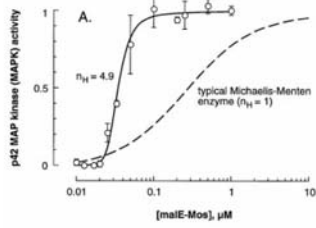
The assumed  $K_m$  values for each reaction were individually varied over the ranges shown, with the assumed  $K_m$  values for the other nine reactions held constant. The effective Hill coefficients were calculated from the steepness of the predicted stimulus/response curves, as described in the text.

<sup>†</sup>The  $K_m$  value for reaction 7 has been measured to be 300 nM for the phosphorylation of a mammalian MAPK by a MAPKK (N. Ahn, personal communication). All of the other  $K_m$  values were initially assumed to be 300 nM as well.

Table 3. Predicted Hill coefficients for MAPK cascade components assuming one-step (processive) or two-step (distributive) models for the phosphorylation of MAPK and MAPKK

Model	Effective Hill coefficient (nH) predicted for:		
	MAPKKK	MAPKK	MAPK
One-step phosphorylation for MAPKK activation;			
One-step phosphorylation for MAPK activation	1.0	1.3	1.5
One-step phosphorylation for MAPKK activation;			
Two-step phosphorylation for MAPK activation	1.0	1.3	2.0
Two-step phosphorylation for MAPKK activation;			
One-step phosphorylation for MAPK activation	1.0	1.7	3.7
Two-step phosphorylation for MAPKK activation;			
Two-step phosphorylation for MAPK activation	1.0	1.7	4.9

Biochemistry: Huang and Ferrell



B.N. Kholodenko et al./FEBS Letters 414 (1997) 430-434

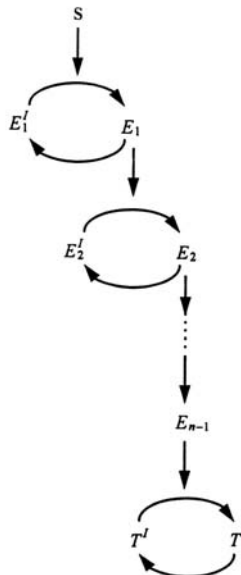


Fig. 1. A simplified scheme of a signal transfer through a signal transduction pathway. At each cascade level only two interconvertible forms are shown. Superscript I denotes inactive forms, e.g.  $E_1^I$  and  $E_1$  stand for inactive and active receptor. The active form ( $E_i$ ) at each level affects the activating and/or inactivating conversion at the subsequent level ( $i+1$ ).

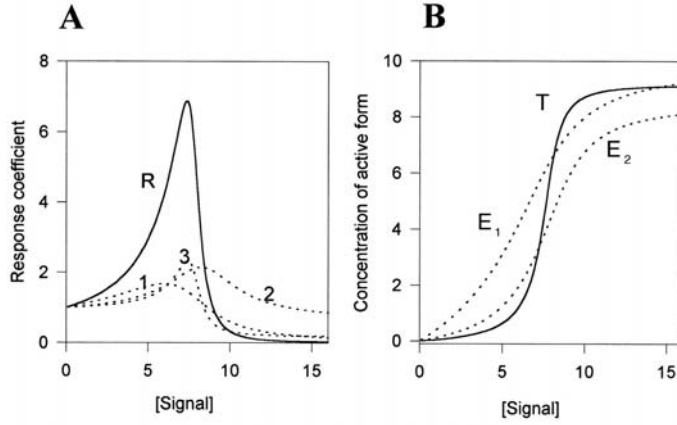


Fig. 3. Signal transduction via a three-level model cascade. A: Dependencies of the local and the total responses on the signal. Dashed lines 1, 2 and 3 correspond to the local responses. The total response of the target ( $R_T^2$ ) is shown by the solid line. For simplicity, the kinases and phosphatases at each cascade level were assumed to follow Michaelis-Menten kinetics,  $v_{A_i} = k_i^{act} \cdot E_{i-1} / (1 + E_i^2 / K_{mK}^2)$ ,  $v_{P_i} = V_i^{max} / (1 + E_i / K_{mP}^2)$ . The activity of the kinase at the first level was assumed to be proportional to the concentration of the signal, i.e.  $E_0 = S$ . The parameter values were (dimensionless units):  $e_1 = (E_1 + E_1^2) = 10$ ;  $k_1^{act} = 1$ ,  $K_{mK}^1 = 1$ ,  $K_{mP}^1 = 4$ ,  $V_1^{max} = 10$ ;  $e_2 = (E_2 + E_2^2) = 10$ ;  $k_2^{act} = 1$ ,  $K_{mK}^2 = 0.5$ ,  $K_{mP}^2 = 3$ ,  $V_2^{max} = 10$ ;  $e_3 = T + T^2 = 10$ ,  $k_3^{act} = 1.5$ ,  $K_{mK}^3 = 1$ ,  $K_{mP}^3 = 2$ ,  $V_3^{max} = 10$ . B: Increase in the sensitivity of the activation state to changes in the signal with the level of the cascade. The dependencies of the concentrations of  $E_1$  (---),  $E_2$  (- - -) and  $T$  (—) on  $S$  are shown.